Basement, Crawlspace, and Slab-on-Grade Thermal Performance

P.H. Shipp
ASHRAE Member

ABSTRACT

The use of improved insulation and sealing procedures on the above-ground residential envelope has increased the importance of ground-coupled coupled heat exchange in the total envelope energy load. Historically, these loads have been estimated using steady-state techniques, which simplify the multidimensional nature of the heat flow paths and neglect the substantial thermal mass of the soil. These simplified procedures are best suited for estimating winter heat losses in climates with more than 3,000 annual heating degree-days. They have proven unsatisfactory, however, in estimating ground-coupled thermal performance during the cooling season for all climates. A transient, two-dimensional finite-difference program has been developed for analyzing heat transfer through the exterior envelope of the ground-coupled elements in a residence. Detailed thermal data obtained from three conditioned basements in Granville, Ohio over a 20-month monitoring period were used for experimental validation of the computer model.

Using the transient analysis, a survey of the annual heating and cooling loads of a variety of basement, crawlspace, and slab-on-grade constructions was conducted. A range of climates representative of the contiguous United States was examined with each test configuration. The results are presented as a series of regression equations that express annual or seasonal energy loads as functions of insulation thermal resistance and local climatological data. Location as well as thermal resistance of the insulation is shown to have important consequences.

Paul H. Shipp, Senior Engineer, Research and Development Division, Owens-Corning Fiberglas Corporation, Technical Center, Granville, OH.

INTRODUCTION

The Energy Performance Design System (EPDS) is a simplified procedure for evaluating whole-house energy demand based upon the thermal performance of individual building elements. In the course of its development, more complex transient analyses were used to catalog the thermal characteristics of a variety of building components for the range of climates representing the contiguous United States. This paper describes the construction of the data-base for earth-contact elements in residential applications.

Until recently, energy loads related to basement, crawlspace, and floor-slab envelope loss have received only cursory attention. Heat-transfer calculations traditionally utilized greatly simplified models broadly encompassing many design configurations.[1-5] The economics of inexpensive energy were chiefly responsible for the acceptance of such abbreviated analytical techniques. Earth-contact heat losses accounted for only a minor proportion of the exterior envelope loads because of the overall use of relatively low levels of insulation. Low-cost energy also allowed a larger margin for error in residential heat-loss calculations at the expense of more detailed analyses.

Increased emphasis upon energy conservation and the subsequent introduction of improved sealing and insulation practices has placed the subject in a new perspective. The proportion of the total envelope load attributable to an uninsulated conditioned basement in Columbus, Ohio, can rise from 25 to 67 percent when only the above-grade part of the house is insulated.[6] These values can vary with geometry, climate, or a number of other factors. This example illustrates, however, that basements and crawlspaces are major components in the energy balance of modern, energy-efficient houses.

Several improved techniques for calculating earth-contact heat transfer have been introduced into literature recently. Frequently, these are steady-state analogues to heat flow through the earth-contact envelope. Ground heat flow is defined one-dimensionally to permit adaptations of the concentric heat flow method introduced by Boileau and Latta,[7-9] or analogue computer studies.[10] The presence of the soil is factored into the heat flow equation by dividing the wall into sections, each being assigned a thermal resistance corresponding to its depth below the ground surface added to the local wall resistance. Steady-state methods can be used to advantage in determining seasonal or monthly heating loads. Failure to account for massiveness in the surrounding soil, however, renders them inappropriate for computing cooling-season loads, annual loads, or conditions defined by relatively rapid transients.[11] The assumption of one-dimensional heat flow neglects thermal bridging and fails to detect corner effects. This can particularly lead to errors when dealing with partially insulated structures.[12-14]

Swinton and Platts correlated experimentally determined basement heat losses with heating degree-days for different levels of insulation.[15] The procedure retains the simple mathematical format characteristic of steady-state methods without the inherent limitations in accuracy. The statistical analysis of empirical data, however, constrains its application within the conditions defined by the sample population. The difficulty of obtaining such data is a major encumbrance to extending this procedure over a range of climates and structural configurations. In addition, as will be shown later, heating degree days are necessary but not sufficient for describing annual loads in climates warmer than the Canadian sites studied in the paper.

A more flexible alternative is to construct a numerical model of the ground heat flow regime. Transient, multidimensional computer modeling permits a detailed description of the building configuration with a comprehensive accounting of the energy fluxes. This provides the most accurate analytical

means available for determining heating and cooling loads of earth-coupled building elements. Finite-difference and finite-element numerical techniques have been successfully applied to a variety of earth-coupled building heat-transfer problems and their accuracy demonstrated.[16-19] A major disadvantage lies in the cost and complexity of implementing such programs. Consequently, they remain primarily research tools which are largely unsuited for use in residential design applications.

In order to provide an accurate and consistent analytical description of the broad spectrum of conditions in the EPDS data base, transient-finite-difference and response-factor computer models were developed for the earth-coupled and above ground building elements. A variety of construction details were chosen to reflect current practices. In like manner, studies ranged from the uninsulated structure to the highest insulation levels judged practical for each case. Annual energy requirements were determined from the heating and cooling season loads for the various basement, crawlspace, and slab-on-grade configurations. For each configuration, regression equations have been developed presenting the results as a function of the wall thermal resistance, heating degree-days, and cooling degree-days.

DESIGN CONFIGURATIONS

Twenty-six earth-contact cases were examined, each representing a unique insulation configuration for the particular construction type. These cases, which are listed in Tab. 1, include 12 basement, 10 crawlspace, and 4 slab-on-grade groups.

The basement analyses included conditioned and unconditioned basements. For each of these, insulating both the full wall and only the top half of the wall were studied. Deep and shallow basement configurations were considered as well as masonry block and all-weather wood foundation (AWWF) wall constructions. The floor of the deep basement is 82 in. (208 cm) below grade with 12 in. (30 cm) of the wall exposed above the ground surface. In the shallow basement, the floor is 50 in. (127 cm) below grade and 44 in. (112 cm) of the wall extends above grade level. The basement floor is an uninsulated 4 in. (10 cm) concrete slab in all cases.

Basement wall insulation can cover either the interior surface, the exterior surface, or, in the case of AWWF construction, it can be installed inside the wall structure. Shipp and Broderick demonstrated that if the wall is insulated over its full height, numerical predictions of basement heat loss differ by less than five percent between interior and exterior insulation placements.[20] With only the upper half of the wall insulated, a 10% variation was observed when comparing the two configurations. These differences represent a minor perturbation of the whole house energy budget, typically less than three percent. It was therefore determined that the added complexity of separating interior and exterior insulation on masonry basement walls is not required in a general predictive model.

A 32 in. (81 cm) foundation wall extending 12 in. (30 cm) above grade level was employed for the basic crawlspace geometry. The crawlspace floor was bare soil. Footings were set at the local soil frost penetration depth where the minimum depth of 20 in. (51 cm) was exceeded. Both masonry block and AWWF wall construction were examined. The house floor above the crawlspace is constructed of nominal 2" x 10" (4 cm by 24 cm) joists installed on 16 in. (41 cm) centers underlaying a 0.75 in. (2 cm) plywood subfloor with carpet and pad. The house floor was insulated above the vented crawlspace; however, a variety of wall and floor insulation configurations were examined for unvented crawlspaces.

Floating slab-on-grade construction is employed in the floor slab model. The outer edge of the 5 in. (13 cm) slab rests on a ledge cast into the poured concrete foundation wall. Insulation is placed horizontally over the ground surface beneath the slab perimeter in the first two cases. In this configuration, R-4 (RSI-0.7) insulation is installed in the joint between the slab and the foundation to control edge losses. The last two cases incorporate vertical insulation placed around the outside of the foundation. Insulation extends down the exterior face of the foundation 2 ft (61 cm) and 4 ft (122 cm) from the top of the slab.

CALCULATION PROCEDURES

Heat transfer through the earth coupled building envelope and surrounding soil was computed by means of a transient two-dimensional finite difference program. The basic routine utilizes the energy conservation equation restricted to conduction heat transfer:

$$\nabla\cdot(k\,\nabla T) = \rho c\,\frac{\partial T}{\partial t} \qquad (1)$$

where

T = temperature of the medium
ρ = density
c = specific
k = thermal conductivity
t = time

In two-dimensional rectangular coordinates, this expands to:

$$\frac{\partial}{\partial x}\left(k\,\frac{\partial T}{\partial x}\right) + \frac{\partial}{\partial y}\left(k\,\frac{\partial T}{\partial y}\right) = \rho c\,\frac{\partial T}{\partial t} \qquad (2)$$

A finite-difference representation of Eq 2 was obtained using standard numerical techniques. The resulting algorithm is a fully implicit central differencing procedure. A description of the model with a discussion of its inherent assumptions can be found in Refs 21 and 22.

Published ASHRAE data provided the film coefficients and solar insolation values.[23,24] Interior convection and radiation effects for the wall and floor boundary conditions are combined in their respective film coefficients. The exterior film coefficients correspond to wind speeds of 15 mph (6.7 m/s) during winter and 7.5 mph (3.4 m/s) during summer. A mean value is used during the spring and fall.

Daily temperature and heat-flux distributions are computed using outdoor air temperatures provided by NOAA Test Reference Year (TRY) weather data. The temperature at time t and depth x within a semi-infinite solid of thermal diffusivity α, and whose surface is subjected to a sinusoidal temperature wave of annual periodicity, τ, provides the soil temperature boundary condition at the bottom of the calculation domain:

$$T(x,t) = AO + BO\,\exp\left(-x\sqrt{\frac{\pi}{\alpha\tau}}\right)\cos\left(\frac{2\pi t}{\tau} - x\sqrt{\frac{\pi}{\alpha\tau}}\right) \qquad (3)$$

The coefficients AO and BO are evaluated from the data of Kusuda and Achenbach.[25]

The measured thermal conductivity in damp porous media such as soil is actually an apparent conductivity, not a true thermodynamic property. It

represents a composite of heat conduction between soil grains and energy fluxes associated with moisture and vapor transport within the pores of the soil matrix. Thus, the apparent thermal conductivity is a function of soil composition, moisture content, temperature, and their respective gradients. [26,27]

Soil thermal conductivities generally vary from 0.6 to 1.2 Btu/hr· ft·°F (1.0 to 2.1 W/m · K) with moisture content providing the greatest source of variation under field conditions. Within this range, specific characterization of the soil behavior requires precise knowledge of the local environment and microclimate at the particular site. Detailed description of soil parameters therefore provides no real advantage over the use of average soil properties when representing a broad spectrum of geographic locations in a general utility program.

In order that the results more accurately reflect differences in climate and building design, a single set of soil properties was adopted for all cases. A silty loam clay with 116 lb /ft^3 (1856 kg/m^3) dry density, 21 % moisture content, an apparent thermal conductivity of 0.86 Btu/hr·ft· °F (1.48 W/m·K), and 0.32 Btu/lb ·°F (1331 J/kg·K) specific heat was selected.

The basic soil heat transfer algorithms were checked by comparing predicted envelope heat fluxes with those measured at three test basements in Granville, Ohio. The three 23.7 ft by 22 ft c 7.8 ft (7.2 m by 6.7 m by 2.4 m) basements differ only with respect to the amount of insulation installed in each. The control basement has uninsulated masonry block walls with a concrete floor slab 6.8 ft (2.1 m) below grade. The walls of the second basement are insulated over the interior surface with R-11 (RSI-1.9) fiberglass batts installed in a nonstructural stud wall framework. Gypsum wallboard completes the installation. The third basement has 6 lb/ft^3 (100 kg/m^3) fiberglass board covering the exterior wall surface with a nominal thermal resistance of R-10 (RSI-1.8). The rigid fiberglass board serves both as thermal insulation and as a drainage medium to keep water away from the basement wall.[28] Drain tile at the base of the insulation prevents water from accumulating inside the insulation. Heat flux transducers mounted 4 in., 16 in., 34 in., 52 in., 70 in., 88 in., (0.1 m, 0.4 m. 0.9 m, 1.3 m, 1.8 m, and 2.2 m) from the top of the walls measure the heat-flux profile through the interior surface of the north and south walls. Heat flux transducers placed 10 in., 65 in., 130 in., (0.3 m, 1.7 m, and 3.3 m) from both walls determine floor heat fluxes. All three basements were maintained at a uniform 76 °F (24 °C) interior air temperature. Continuous monitoring of the basements began during October, 1980. Prior to that time, the basements were unconditioned.

Average monthly north and south wall heat fluxes predicted by the transient two-dimensional model for the three basements are plotted in Figs. 1a and 1b, respectively, from October, 1980, through May, 1982. Predicted floor heat fluxes for the same period are graphed in Fig. 1c. The corresponding measured data are shown by unconnected symbols. The computer model tracks well with the measured data following a brief startup period. The maximum wall variance during 1981 was a 0.9 Btu/hr· ft^2 (2.8 W/m^2) deviation from the January measured value of 7.4 Btu/hr·ft^2 (23.4 W/m^2) on the uninsulated south wall. On average, the predicted monthly wall heat fluxes differed by less than 0.1 Btu/hr·ft^2 (0.3 W/m^2) throughout the year for the three basements.

The floor data exhibits larger deviations between measured and predicted values although the general agreement remains good. For example, beginning in February, one basement showed a marked increase in floor heat loss during both 1981 and 1982. These variations correlate with seasonal fluctuations in the local water table level and reflect that house's 6 and 13 ft (1.8 m, 4.0 m) lower elevation relative to the other two houses. Over the 315 ft (96 m) length of the test site, the average variation in water table depth is 6 ft (1.8 m). The highest recorded level was 5.4 ft (1.6 m) below the ground

surface in March, 1982, the lowest level having been recorded at 5.3 m (18 ft) in August, 1981.

For vented crawlspaces, the house floor is the lower boundary of the conditioned space's exterior envelope and should be insulated. Insulating crawlspace walls or the ground surface provides little benefit because of air infiltration through the ventilation ports, although the crawlspace remains a thermal buffer for the conditioned space. Response-factor methodology coupled with an explicit finite-difference model of ground-heat transfer was utilized for the transient analysis of the floor above a vented crawlspace.[29]

RESULTS AND DISCUSSION

The annual heating and cooling season envelope loads for the 26 test cases were calculated for a broad range of insulation levels using the above procedures. Conditioned space temperatures were maintained at 73 F (22.8 C) throughout the year. Balance points for the heating and cooling load splits were determined by means of whole-house simulations. The house balance point reflects the myriad thermal interactions among various building elements. Hence, assumptions regarding the house configuration are implicit in the assignment of this parameter.

The basic stipulation of a balanced overall building design was adopted. Equal consideration was given to the thermal characteristics of each element in the residence. For example, the balance point assigned for studying a well insulated basement was drawn from a house whose above-ground elements are also well insulated. Using an uninsulated house's balance point in this case would violate the criterion of a balanced design. For consistency, base-case data were compiled by examining a single test house insulated to comply with current HUD minimum standards for each region. Insulation levels judged to exemplify excellent energy efficiency defined the upper limits. Linear interpolation established the balance points for intermediate insulation levels.

The desired spectrum of climates was represented by five test cities. The cities and their corresponding heating degree-days (HDD) and cooling degree-days (CDD) are listed in Tab. 2. Although individual balance points varied with insulation levels for calculating envelope loads, the following regression equations utilize HDD and CDD based upon a standard 55 F (12.8 C) balance point.

Figure 2 plots the annual energy use predicted for a conditioned basement whose masonry walls are insulated over their full height (case B-A). Curves representing different levels of insulation ranging from an uninsulated wall to R-38 (RSI-6.7) insulation over the full height of the wall are shown. The observed pattern is representative of the general findings. Annual and seasonal loads are expressed in terms of energy usage per unit perimeter. This format was selected because the perimeter region dominates envelope losses for shallow earth-sheltered elements. The sole deviation from this rule is the floor over a vented crawlspace (case F) for which the data are presented as energy per unit area.

A 30 ft by 40 ft (9 m by 12 m) rectangular plan area specified the ratio of wall and floor data for the perimeter losses. In an uninsulated basement of the same dimensions, corner effects can produce nine percent higher envelope losses than are indicated solely by center wall fluxes.[31] This is because the uninsulated wall's thermal resistance is principally derived from the surrounding soil in which the corners are dull fins. Even moderate levels of insulation dominate the wall's thermal resistance, however, and corner effects become negligible. Corner effects were therefore omitted, the primary

consequence being to underestimate uninsulated envelope loads. Consequently, the results conservatively estimate the benefits of insulating earth-contact structures.

To provide a more compact and accessible presentation of the data, the annual and seasonal energy load curves for each of the 26 test cases were transformed into linear regression equations. The objective of the regression analysis was to identify critical parameters in such away that the same basic equation, utilizing a minimum number of coefficients, could be applied to all cases. Heating loads, cooling loads, and total annual loads were examined independently although the same model was ultimately found to work well for all three. Wall or floor thermal resistance (R), conductance (1/R), HDD, CDD, and their associated quadratic and cross-product terms were considered initially. Quality of fit was judged on the basis of maximizing the multiple correlation coefficient (R^2) and minimizing the coefficient of variation. Residuals were plotted against predicted values and heating degree-days for each case to insure against unacceptably large or systematic errors. A seven variable model best satisfied the given constraints:

$$Q = B0 + B1/R + B2*(HDD/100) + B3*(CDD/100) + B4*(HDD/100)/R + B5*(CDD/100)/R + B6*(HDD/100)*(CDD/100) + B7*(HDD/100)*R \quad (4)$$

Q represents annual envelope load, heating season load, or cooling season load depending upon the choice of coefficients B0 through B7. The coefficients for the annual energy load regressions are listed in Tab. 3. The regression coefficients resulting from fitting the heating-season data to the above model are given in Tab. 4, whereas the cooling season regression coefficients can be found in Tab. 5. The regression coefficients in Tabs. 3 through 5 give the annual or seasonal energy loads per unit perimeter, (Btu/ft). The sole exception to this is case F, an insulated floor over an uninsulated crawlspace. For this latter case, annual and seasonal loads are given per unit area, (Btu/ft^2). As noted earlier, this follows the convention that where earth coupling is the principle heat transfer condition the perimeter zone dominates the total heat transfer. It should be emphasized, however, that while the results have been normalized in terms of a perimeter weighting, the total floor and wall areas of each configuration were used for deteriming the loads. Thermal resistance, R, describes the total resistance of the insulated structure, not just the amount of insulation. Hence, an uninsulated masonry wall is R-1.04. Annual heating degree days (HDD) and cooling degree days (CDD) are determined for a balance point temperature of 55 deg. F, as shown in Tab. 2. For the regression equations, HDD and CDD are divided by 100 to minimize truncation errors in the cross product term (B6). The model fits the data well, as shown by a mean multiple-regression coefficient for the annual and heating-season loads of 0.997 with 0.001 standard deviation and a minimum value of 0.995. Cooling-season regressions yielded a mean R^2 of 0.978 with 0.014 standard deviation, giving marginally lower compliance for the 26 cases.

Because the model is fitted to physically deterministic data, the apparent precision of the proportionality of energy fluxes to conductance, heating degree-days, and cooling degree-days is not unexpected. The regressions use only one of several possible models, however, and should not be interpreted as definitive physical models. The following paragraphs demonstrate that numerous transient and two-dimensional characteristics are interacting in each case. The regression equations represent the composite effect of these phenomena and can mask the individual significance of each.

As indicated in Fig. 2, the value of higher insulation levels is greatest in colder climates. Although a net reduction in total energy usage can be attributed to each incremental increase in insulation level, only minor

improvements occur in the warmest climates. This was observed to be characteristic of earth-coupled structures in cooling-season-dominated climates. In these regions, some insulation is warranted because of undesireable heat gains through the upper portion of the basement or crawlspace wall during warm periods. Beneficial heat losses occur concurrently at the base of the wall and through the floor, however. Reduced losses to the surrounding soil can therefore counterbalance the decreased heat gains for high insulation levels in very warm climates.

In temperate climates such as Dallas or St. Louis, an insulated basement can reduce the total house envelope load. Such conditions are indicated by negative annual energy requirements in Fig. 2. By insulating the walls but not the floor, the relatively benign soil environment exerts a stabilizing effect upon basement temperatures. Insulated basements can also contribute significantly to reducing house loads in more severe winter climates by providing a stable, moderate environment for a large percentage of the house's useful floor area.

The thermal performance of five insulation configurations for an unvented crawlspace with masonry walls is shown in Fig. 3. Annual energy loads are plotted for an uninsulated crawlspace, for R-11 (RSI-1.9) and R-30 (RSI-5.3) wall insulation alone, and for R-11 and R-30 batts covering the wall and 8 ft (2.4 m) of the floor perimeter. The crawlspace with R-30 wall insulation alone displays marginally lower requirements than the combined R-11 wall and floor insulation case.

The similarity of these two cases derives from the multidimensional nature of earth-contact heat flow. During the heating season, the reduced wall heat loss resulting from the addition of insulation produces colder soil temperatures near the basement. Floor perimeter losses consequently increase. The converse situation of wall losses increasing because of reduced floor heat loss can also occur.

Sensitivity to this phenomenon can be influenced by selection of the foundation material. In masonry construction, the wall represents a low-resistance path, which acts as a fin enhancing heat transfer from the adjacent soil to the outside air during winter. This vertical thermal bridging path reduces the sensitivity of soil temperatures to wall insulation levels and, hence, reduces dependence of floor losses upon wall insulation levels. Crawlspace floor perimeter insulation therefore complements wall insulation very effectively in masonry foundations, and, as indicated by Fig. 3, different combinations can achieve similar results.

In contrast, the insulated wood-frame structure of an AWWF crawlspace does not constitute an effective cooling fin. Local soil temperatures, wall heat losses, and floor heat losses are more intimately related with an interdependence demonstrated in the regression coefficients for cases C-G, C-H, and C-I. The three equations are nearly identical in Tab. 3, revealing that decreased floor losses following the addition of floor perimeter insulation are compromised by increased wall losses. Hence, efforts should focus primarily upon insulating the walls of unvented AWWF crawlspaces.

Compared with masonry block basement wall construction, an AWWF basement exhibits smaller energy loads when low levels of insulation are used. This is mainly due to the higher thermal resistance of the uninsulated AWWF wall (R-2.5 vs R-1.04). While the thermal fin effect discussed above is a contributing factor, the greater depth of the basement floor reduces its sensitivity to wall characteristics. Therefore, differences between the two basement constructions diminish rapidly as insulation is added.

The effect of arranging the same amount of insulation in different configurations below the perimeter of a slab-on-grade floor is illustrated in

Fig. 4. The best performance is derived from insulating the outer 4 ft (1.2 m) of the slab perimeter as opposed to placing twice the thermal resistance below the outer 2 ft (0.6 m) of the slab or half the thermal resistance below the outer 8 ft (2.4 m). These differences are minor, however, when compared with the improvements over an uninsulated slab.

The difficulty of controlling edge losses and insuring an unbroken insulating envelope underneath the slab, as well as greater flexibility in construction scheduling, favor placing slab perimeter insulation over the outside surface of the foundation. The effect of installing vertical exterior insulation on slab floors is shown in Fig. 5. For winter dominated climates, insulation installed to a depth of 4 ft (1.2 m) below the top of the floor slab results in lower energy demands than when the same amount of insulation is installed over the top 2 ft (0.6 m) of the foundation. In warmer climates, however, the 2 ft insulation depth performs as well as the deeper installation. Comparing Figs. 4 and 5, it can generally be concluded that exterior insulation covering the outer surface of the foundation will provide improved thermal performance relative to the same quantity of insulation laid horizontally below the slab perimeter.

CONCLUSIONS

The annual exterior envelope loads were determined for a broad range of insulation levels in each of 26 basement, crawlspace, and slab-on-grade construction configurations. A transient, two-dimensional computer program that computed daily energy fluxes over an entire year was employed for the calculations. Weather data spanned the spectrum of climates representing the contiguous United States.

The multidimensional nature of earth-contact heat transfer was clearly demonstrated by the results. The different test configurations showed that location of the insulation can be as important as the thermal resistance in reducing thermal loads. In general, adding insulation reduced envelope loads for all cases and climates. The benefits accrued are greatest in colder climates, however, with the warmest climates showing a more pronounced point of diminished returns.

Linear regression analysis was employed to present the results of the calculations. A seven-variable model was found to provide the best fit with a minimum number of parameters. The essential parameters for describing earth-contact heat transfer over such a broad climatic range are thermal conductance, heating degree-days, cooling degree-days, and their respective cross product terms. The product of heating degree-days and thermal resistance provided the seventh variable for the model. Quadratic terms and the other possible cross product terms were not found to significantly improve the model.

Program validation was carried out through comparisons with measured basement data. The singular behavior of the basement floors required that the thermal data be supplemented by additional knowledge of local water table fluctuations. This illustrates that predicting earth-contact heat transfer with a high degree of precision is unrealistic in the absence of such detailed information regarding the microclimate. Predictive models should be evaluated with regard to their ability to give plausible, consistent results as well as with respect to comparisons between individual experimental test cases. Complex and extremely detailed models do not necessarily provide more accurate predictions of future building performance because the variability of key parameters and are unsuited for use as general purpose design tools.

REFERENCES

1. F.C. Houghten, S.K. Taimuty, C. Gutherlet and C.J. Brown, "Heat Loss Throught Basement Walls and Floors", ASHVE Transactions 48 (1942), p. 369-384.

2. R.S. Dill, W.C. Robinson and H.E. RObinson, "Measurements of Heat Losses from Slab Floors", U.S., Department of Commerce, Nation Bureau of Standards, Building Materials and Structures, Report BMS 103 (March 1945).

3. H.D. Bareither, A.N. Fleming and B.E. Alberty, Temperature and Heat Loss Characteristics of Concrete Floors Laid on the Ground (Urbana, IL: Small Homes Council, Department of Mechanical Engineering, University of Illinois, 1948).

4. ASHRAE Handbook - 1972 Fundamentals, Chapter 24, p. 377.

5. R.A. Jones, Crawl-Space Houses (Urbana, IL: Small Homes Council, Depatement of Mechanical Engineering, University of Illinois, January 1959), Bulletin 56:39 .

6. P.H. Shipp and T.B. Broderick, "Comparison of Annual Heating Loads for Various Basement Wall Insulation Strategies Using Transient and Steady-State Models", Thermal Insulations, Materials, and, Systems for Energy Conservation in the '80's (Philadelphia, PA: American Society for Testing and Materials, 1983 ASTN STO 789)m o, 455-473.

7. Canada, National Research Council, Division of Building Research, Calculation of Basement Heat Loss by G.G. Boileau and J.K. Latta (Ottawa: National Research Council 1968 Technical Paper 292).

8. ASHRAE Handbook - 1981 Fundamentals, Chapter 25, p. 25.4 - 25.7.

9. American Plywood Association, Advantages and Considerations of Insulating Foundation Walls, Technical Note 2410 (Tacoma, WA: American Plywood Association, 1977).

10. France, Centre Scientifique et Technique du Batiment, Unified Code of Practice, Rules for Calculating Practical Thermal Properties of Structural Components (Paris: Center Scientifique et Technique du Batiment 1975 Rules Th-K77), p. 34-42.

11. Shipp and Broderick, p. 472.

12. Ibid, p. 472.

13. F.S. Wang, "Mathematical Modeling and Computer Simulation of Insulation Systems in Below Grade Applications", Proceedings of the ASHRAE/DOE-ORNL Conference, Thermal Performance of the Exterior Envelopes of Buildings (New York: ASHRAE, 1981), p. 461.

14. P.H. Shipp, "Natural Convection Within Masonry Block Basement Walls", ASHRAE Transactions 89:1 (1983).

15. M.C. Swinton and R.E. Platts, "Engineering ,Method for Estimating Annual Basement Heat Loss and Insulation Performance", ASHRAE Transactions 87:2 (1981).

16. P.H. Shipp, E. Pfender and T.P. Bligh, "Thermal Characteristics of a Large Earth-Sheltered Building", Parts I and II, Underground Space 6 (July/August 1981), p. 53-64.

17. R.F. Szydlowski and T.F. Kuehn, "Analysis of Transient Heat Loss in Earth-Sheltered Structures", Earth-Sheltered Building Design Innovations, ed., L.L. Boyer (Stillwater, OK: Architectural Extension, Oklahoma State University, 1980), p. III-25.

18. F.S. Wang, p. 456-471.

19. P.C. Deacon, "Glass Fibre as a Draining Insulation System for the Exterior of Basement Walls", Thermal Insulation, Materials, and Systems for Energy Conservation in the '80's (Philadelphia, PA: American Society for Testing and Materials, 1983 ASTM STP 789), p. 413-434.

20. Shipp and Broderick, p. 463.

21. Shipp, Pfender, and Bligh, Part II.

22. P.H. Shipp, EPDS Documentation: Basement, Crawlspace, and Floor Slab Insulation Study (Granville, OH: Owens-Corning Fiberglas, Technical Center, 1982 TR 82-T-255).

23. ASHRAE Handbook - 1981 Fundamentals, Chapter 23, p. 23.12-23.13.

24. Ibid, Ch. 27, p. 27.19 - 27.36.

25. T. Kusuda and P.R. Achenbach, "Earth Temperature and Thermal Diffusivity at Selected Stations in the United States", ASHRAE Transactions 71:1 (1965) p. 61-75.

26. J.R. Philip and D.A. deVries, "Moisture Movement in Porous Materials under Temperature Gradients", American Geophysical Union Transactions 38:2 (April 1957), p. 222.

27. D.A. de Vries, "Simultaneous Transfer of Heat and Moisture in Porous Media", American Geophysical Union Transactions 39:5 (October 1958), p. 909.

28. P. C. Deacon, p. 413-434.

29. P.M. Frase and M.F. McBride, OCF-2 User's Manual (Granville, OH: Owens-Corning Fiberglas, Technical Center, 1981 TR 81-T-62).

30. M.F. McBride, "Development of a Simplified and Manual Energy Calculation Procedure for Residences", Proceedings of the ASHRAE/DOE Conference, Thermal Performance of the Exterior Envelopes of Buildings II (New York: ASHRAE, 1983).

31. Swinton and Platts, p. 2.

TABLE 1

Earth Contact Building Envelope Configurations.

Case	Description
B-A	Conditioned basement, fully below grade, 8 in. block or concrete, insulation covers entire wall.
B-B	Conditioned basement, fully below grade, 8 in. block or concrete, insulation covers top half of wall.
B-C	Conditioned basement, half below grade, 8 in. block or concrete, insulation covers entire wall.
B-D	Conditioned basement, half below grade, 8 in. block or concrete, insulation covers top half of wall.
B-E	Unconditioned basement, fully below grade, 8 in. block or concrete, insulation covers entire wall.
B-F	Unconditioned basement, fully below grade, 8 in. block or concrete, insulation covers top half of wall.
B-G	Unconditioned basement, half below grade, 8 in. block or concrete, insulation covers entire wall.
B-H	Unconditioned basement, half below grade, 8 in. block or concrete, insulation covers top half of wall.
B-I	Conditioned basement, fully below grade, all-weather wood foundation, (2 x 8) or (2 x 10) 12 in. on center, insulated full wall height.
B-J	Conditioned basement, half below grade, all-weather wood foundation, (2 x 8) or (2 x 10), 12 in. on center, insulated full wall height.
B-K	Unconditioned basement, fully below grade, all-weather wood foundation, (2 x 8) or (2 x 10), 12 in. on center, insulated full wall height.
B-L	Unconditioned basement, half below grade, all-weather wood foundation, (2 x 8) or (2 x 10), 12 in. on center, insulated full wall height.
C-A	Unvented crawlspace, 8 in. block or concrete, batt insulation over wall interior.
C-B	Unvented crawlspace, 8 in. block or concrete, batt insulation over wall and 2 ft of floor perimeter.
C-C	Unvented crawlspace, 8 in. block or concrete, batt insulation over wall and 4 ft of floor perimeter.
C-D	Unvented crawlspace, 8 in. block or concrete, exterior rigid board insulation covering top 2 ft of wall.

C-E Unvented crawlspace, 8 in. block or concrete, exterior rigid board insulation covering top 3 ft of wall.

C-F Unvented crawlspace, 8 in. block or concrete, exterior rigid board insulation covering top 4 ft of wall.

C-G Unvented crawlspace, all-weather wood foundation, insulation in wall only.

C-H Unvented crawlspace, all-weather wood foundation, insulation in wall and over 2 ft of floor perimeter.

C-I Unvented crawlspace, all-weather wood foundation, insulation in wall and over 4 ft of floor perimeter.

S-A Slab floor, 5 in. concrete slab, insulation placed horizontally below 2 ft of slab perimeter, R-4 edge insulation.

S-B Slab floor, 5 in. concrete slab, insulation placed horizontally below 4 ft of slab perimeter, R-4 edge insulation.

S-C Slab floor, 5 in. concrete slab, insulation placed vertically over foundation exterior surface to 2 ft below top of slab.

S-D Slab floor, 5 in. concrete slab, insulation placed vertically over foundation exterior surface to 4 ft below top of slab.

F Insulated floor over unconditioned space.

TABLE 2

Climate Descriptors for the Five Test Cities, 55 Deg. F (12.8 Deg. C) Degree Day Balance Point.

City	Heating Degree-Days	Cooling Degree-Days
Bismarck, ND	6963 (3868)	1603 (891)
Minneapolis, Mn	5995 (3331)	2134 (1186)
St. Louis, Mo	3239 (1799)	3064 (1702)
Dallas, Tx	1000 (556)	4833 (2685)
Miami, Fl	18 (10)	7715 (4286)

TABLE 3

Regression Coefficients for Annual Energy Loads.

ANNUAL LOAD = B0 + B1/R + B2*(HDD/100) + B3*(CDD/100) + B4*(HDD/100)/R +
B5*(CDD/100)/R + B6*(HDD/100)*(CDD/100) + B7*(HDD/100)*R

Case	B0	B1	B2	B3	B4	B5	B6	B7
B A	-65182.0	234866.6	4790.72	958.03	2281.77	-2393.58	-50.0196	-56.5746
B B	-94473.0	284276.6	6676.81	1457.07	128.20	-3169.52	-53.6387	-49.4376
B C	-79236.1	502943.3	4883.92	1178.62	4919.19	-5150.88	-30.3211	-61.6059
B D	-69975.0	484011.5	7388.99	1257.28	2190.57	-5115.63	-20.7603	-59.4121
B E	-75309.2	55853.8	3564.20	1215.79	558.15	-243.44	-37.3676	-34.6162
B F	-99601.3	92164.0	4425.44	1767.55	-377.23	-976.40	-43.0632	-27.1896
B G	-68539.3	124074.6	3814.87	1115.86	696.97	-1078.12	-34.5367	-42.0774
B H	-86574.9	146346.1	4800.06	1682.58	-369.87	-1727.51	-36.4247	-28.0835
B I	-32147.2	57721.5	3310.52	-88.28	4885.60	1422.47	7.3460	-81.7491
B J	-60789.9	205241.5	3568.09	384.79	8998.58	333.74	25.7463	-93.1215
B K	-17953.0	-10908.3	2695.16	-45.24	1412.21	1147.56	-16.9808	-51.3298
B L	-28032.8	46302.7	3065.68	168.02	2091.85	626.09	-13.1620	-61.4856
C A	-30164.4	152928.7	3040.22	525.19	1501.60	-1257.31	-37.7920	-24.2951
C B	-35688.0	149632.1	2726.00	531.50	1823.89	-1145.99	-32.0544	-24.5214
C C	-32344.0	143741.1	2512.75	447.44	2046.65	-1026.91	-30.6172	-24.4588
C D	-28872.7	154336.2	3508.65	557.56	1025.51	-1325.30	-40.2136	-19.0358
C E	-32008.7	156081.1	3265.86	518.12	1291.43	-1262.76	-39.2908	-30.8832
C F	-28334.8	154615.4	3180.59	439.15	1392.37	-1209.87	-40.9795	-37.3077
C G	-27837.9	18722.9	2333.54	-231.87	3343.12	1316.84	17.3071	-49.8532
C H	-30430.4	24776.1	2464.87	-203.97	3043.46	1256.59	16.9576	-51.0906
C I	-30715.6	25164.4	2388.37	-207.04	3252.51	1270.46	16.7544	-51.7871
S A	-17908.6	28545.6	2308.29	131.98	-199.80	-326.24	-21.1411	-15.9046
S B	-24165.0	27414.0	2175.99	202.93	-132.40	-305.71	-15.5676	-17.3892
S C	-17780.2	47045.9	2026.07	25.55	-95.09	-419.67	-16.4860	-6.8562
S D	-14712.4	47912.2	1941.40	-27.16	-1.08	-408.33	-17.9179	-13.9386
F	-899.0	12732.4	199.17	19.51	438.83	-68.75	-1.9447	-3.1601

TABLE 4

Regression Coefficients for Heating Season Loads.

HEATING LOAD = B0 + B1/R + B2*(HDD/100) + B3*(CDD/100) + B4*(HDD/100)/R +

B5*(CDD/100)/R + B6*(HDD/100)*(CDD/100) + B7*(HDD/100)*R

Case	B0	B1	B2	B3	B4	B5	B6	B7
B A	15752.9	264922.9	4232.81	-211.94	2671.15	-3290.77	-17.1404	-50.4085
B B	44077.0	246476.3	5608.13	-582.42	1097.35	-3053.95	-18.8354	-32.8669
B C	6779.5	533930.9	4220.85	-112.92	5520.25	-6620.35	-1.8278	-53.2059
B D	82672.2	443572.0	6169.41	-1105.79	3428.27	-5437.27	5.8481	-41.3263
B E	-15029.5	65053.7	3118.27	195.52	744.88	-820.93	-16.2550	-27.9061
B F	-11773.6	67197.9	3738.85	152.92	76.01	-849.10	-19.8428	-16.9480
B G	-6495.8	122312.6	3326.31	80.85	935.19	-1534.99	-15.6238	-34.4686
B H	4961.4	112838.3	4084.04	-67.67	121.66	-1411.82	-18.0038	-18.0098
B I	-8556.0	26793.6	2883.67	87.47	6547.92	189.90	34.0053	-72.5996
B J	-44779.5	151715.7	3029.84	538.28	11202.00	-1107.51	60.0601	-82.0974
B K	-6404.9	-14326.1	2491.87	76.43	2165.96	314.96	2.3235	-44.7881
B L	-14719.9	17420.7	2750.80	178.61	3173.05	-2.53	10.3570	-54.1062
C A	-13061.5	142589.5	2516.88	166.62	2212.99	-1728.66	5.2177	-11.5024
C B	-21001.2	146298.5	2253.11	270.06	2484.96	-1777.22	8.1779	-12.9355
C C	-20050.6	146819.8	2088.04	258.06	2661.36	-1784.28	7.1017	-14.1152
C D	17212.6	132958.3	3240.60	-233.05	1498.54	-1596.26	-9.5144	-19.5189
C E	8289.3	139897.0	3016.01	-116.89	1743.10	-1686.76	-7.9095	-31.7980
C F	8805.5	142789.2	2956.88	-123.25	1816.18	-1724.70	-10.1840	-38.4937
C G	5147.3	1937.7	1915.68	-87.40	4463.67	448.88	28.7724	-38.0732
C H	6350.7	-1461.2	2016.99	-103.02	4230.44	495.90	28.4942	-38.5065
C I	4369.8	3243.9	1963.17	-77.51	4384.10	437.13	28.3213	-39.8001
S A	24350.8	19207.4	2041.88	-315.56	-27.85	-221.21	-4.4759	-9.2073
S B	17325.3	20743.1	1943.58	-224.61	22.27	-240.88	-1.6530	-11.6179
S C	21439.0	35623.1	1912.16	-282.59	79.99	-403.17	-1.7725	-7.8271
S D	18412.0	42527.7	1880.88	-241.71	122.59	-492.12	-3.1001	-15.4857
F	2362.6	23496.2	181.54	-31.74	413.69	-291.89	-1.5868	-3.4443

TABLE 5

Regression Coefficients for Cooling Season Loads.

COOLING LOAD = B0 + B1/R + B2*(HDD/100) + B3*(CDD/100) + B4*(HDD/100)/R +
B5*(CDD/100)/R + B6*(HDD/100)*(CDD/100) + B7*(HDD/100)*R

Case	B0	B1	B2	B3	B4	B5	B6	B7
B A	-80934.9	-30056.3	557.92	1169.97	-389.38	897.20	-32.8792	-6.1645
B B	-138550.0	37800.3	1068.67	2039.50	-969.15	-115.56	-34.8033	-16.5707
B C	-86015.5	-30987.7	663.07	1291.53	-601.06	1469.47	-28.4933	-8.4001
B D	-152647.2	40439.5	1219.59	2363.07	-1237.70	321.64	-26.6084	-18.0857
B E	-60279.7	-9199.9	445.93	1020.28	-186.73	577.49	-21.1125	-6.7101
B F	-88001.7	25139.0	688.50	1617.95	-456.68	-130.65	-23.1341	-10.3015
B G	-62043.5	1762.0	488.56	1035.00	-238.23	456.86	-18.9129	-7.6089
B H	-92229.6	33743.4	719.34	1760.03	-496.01	-319.72	-18.0756	-10.1198
B I	-23591.2	30927.8	426.86	-175.75	-1662.33	1232.56	-26.6593	-9.1512
B J	-16010.4	53525.8	538.25	-153.49	-2203.42	1441.25	-34.3138	-11.0241
B K	-11548.1	3417.8	203.29	-121.68	-753.75	832.60	-19.3043	-6.5416
B L	-13312.8	28882.0	314.88	-10.59	-1081.20	628.61	-23.5190	-7.3794
C A	-17102.9	10339.2	523.34	358.57	-711.39	471.35	-43.0097	-12.7927
C B	-14686.9	3333.6	472.88	261.44	-661.08	631.23	-40.2323	-11.5858
C C	-12293.4	-3078.7	424.72	189.39	-614.71	757.37	-37.7198	-10.3436
C D	-46085.3	21377.9	268.05	790.61	-473.03	270.96	-30.6992	0.4831
C E	-40298.0	16184.1	249.85	635.01	-451.68	424.00	-31.3813	0.9148
C F	-37140.3	11826.2	223.72	562.39	-423.81	514.83	-30.7955	1.1860
C G	-32985.2	16785.2	417.86	-144.47	-1120.56	867.96	-11.4644	-11.7800
C H	-36781.1	26237.3	447.88	-100.95	-1186.97	760.69	-11.5375	-12.5841
C I	-35085.4	21920.5	425.20	-129.54	-1131.59	833.33	-11.5669	-11.9870
S A	-42259.4	9338.2	266.41	447.53	-171.96	-105.03	-16.6652	-6.6957
S B	-41490.3	6670.9	232.41	427.54	-154.67	-64.83	-13.9145	-5.7713
S C	-39219.2	11422.8	113.91	308.14	-175.08	-16.50	-14.7134	0.9710
S D	-33124.5	5384.5	60.52	214.55	-123.67	83.79	-14.8177	1.5471
F	-3377.2	-9076.9	17.44	52.12	6.99	199.78	-0.2642	0.2828

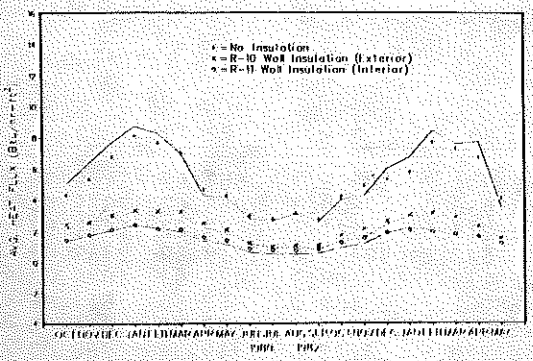

Figure 1a. Average monthly heat loss through the north walls of three test house basements in Granville, OH. Measured data shown as unconnected symbols; predicted values connected by line segments

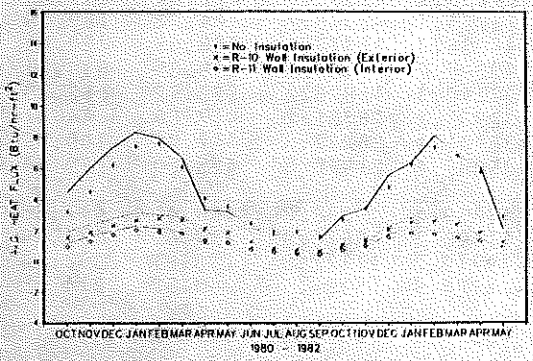

Figure 1b. Average monthly heat loss through the south walls of three test house basements in Granville, OH. Measured data shown as unconnected symbols; predicted values connected by line segments

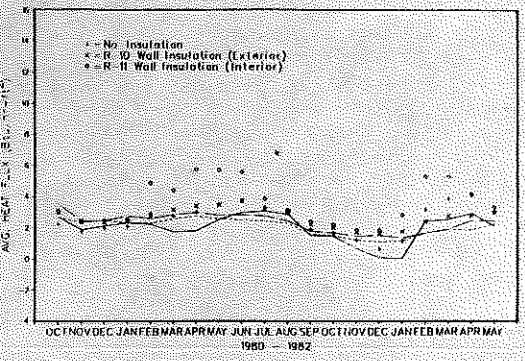

Figure 1c. Average monthly heat loss through the floors of the three test houses in Granville, OH. Measured data shown as unconnected symbols; predicted values connected by line segments

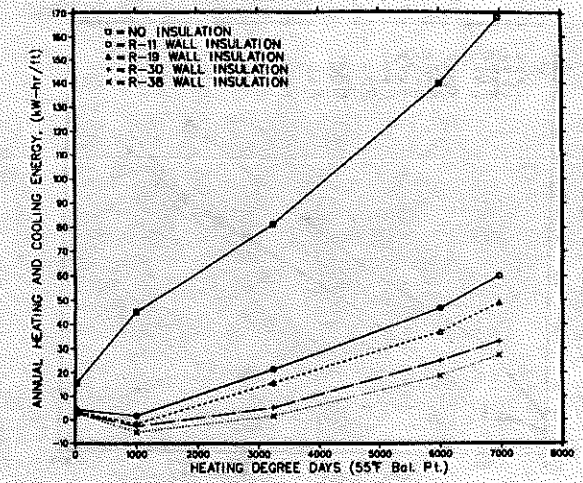

Figure 2. Computed annual basement envelope loads, full wall insulation

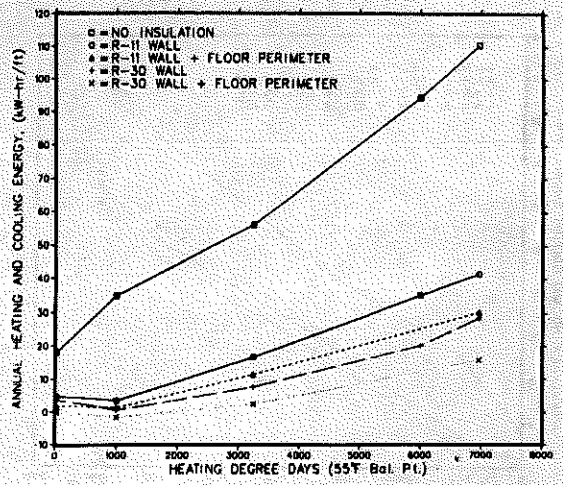

Figure 1. Computed annual crawlspace envelope loads. Wall insulation extends from sill plate to crawlspace floor. Perimeter insulation laid over outer 8 feet of floor

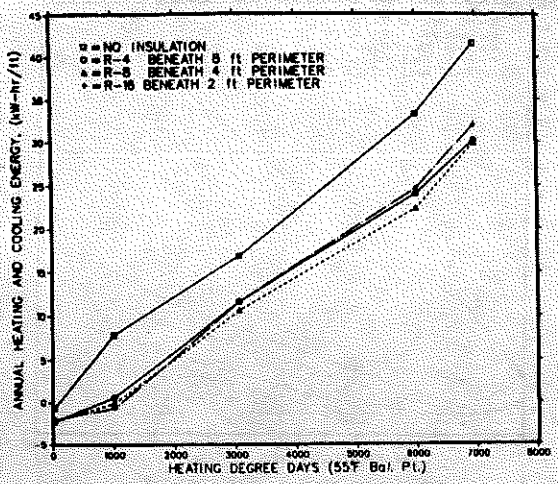

Figure 4. Computed annual loads for slab-on-grade floor with horizontal insulation laid underneath the slab perimeter

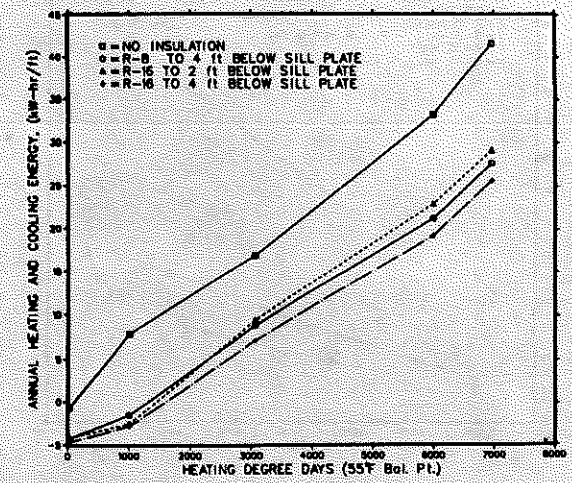

Figure 5. Computed annual loads for slab-on-grade floor with exterior insulation placed vertically over outer face of the foundation

Discussion

B. Renner, Physicist, NBS, Washington, DC: Please give a typical percent difference between experimental values of loads and (1) your finite difference model or (2) traditional steady-state methods?

P. H. Shipp: The heating season loads predicted by the finite difference model for the walls remained within 7% of the measured values for all test cases during the 1981 to 1982 measurement period. In contrast, the seasonal wall losses predicted by the one-dimensional model varied from the finite difference model by 2% for the uninsulated wall and 18% for R-11 (RSI-1.8) full wall insulation. Floor losses produced larger deviations by 25% from the measured results and the one-dimensional model yielded an 80% error.

Cooling season performance showed larger percentage differences between measured and predicted loads although the magnitudes of these deviations were smaller. During the cooling season, the finite difference model underpredicted wall heat losses by 5 to 27% and underpredicted floor losses by 11 to 36%. The one-dimensional model erred by more than 100% in that it predicted heat gains when, in fact, a net heat loss was registered for both the walls and floor.

F. Walter, P.E., Vice-Pres., Tech. Activities, Manufactured Housing Inst., Arlington, VA: In your project, which studied heat loss for a fully insulated crawlspace, did you eliminate ventilation? If so, even though you used a vapor barrier, did you monitor humidity? What were the observations?

P. H. Shipp: Ventilation levels for the insulated crawlspace were limited to anticipated air infiltration rates at the band joist crack around the building perimeter. The experimental validation program studied only the three basements discussed in the text. As such, the crawlspace model is an extension of the finite difference program developed for analyzing basement heat losses and there are no experimental data on crawlspace humidity levels.